Journal of Medicinal Chemistry

Brief Article

pubs.acs.org/jmc

Cyanohydrin as an Anchoring Group for Potent and Selective Inhibitors of Enterovirus 71 3C Protease

Yangyang Zhai,[†,‡] Xiangshuai Zhao,[†,‡] Zhengjie Cui,[†,‡] Man Wang,[†,‡] Yaxin Wang,[§] Linfeng Li,[†,‡] Qi Sun,[∥] Xi Yang,[†,‡] Debin Zeng,[†,‡] Ying Liu,[†,‡] Yuna Sun,[⊥] Zhiyong Lou,[§] Luqing Shang,*[,†,‡] and Zheng Yin*[,†,‡]

[†]College of Pharmacy and State Key Laboratory of Elemento-Organic Chemistry, Nankai University, 94 Weijin Road, Nankai District, Tianjin 300071, China

[‡]Collaborative Innovation Center of Chemical Science and Engineering (Tianjin), Tianjin 300071, China

[§]Laboratory of Structural Biological & Ministry of Education (MOE), and Laboratory of Protein Science, School of Medicine and Life Sciences, Tsinghua University, Beijing 100084, China

[∥]College of Chemistry, and Key Laboratory of Pesticide & Chemical Biology, Ministry of Education, Central China Normal University, Wuhan 430079, China

[⊥]National Laboratory of Macromolecules, Institute of Biophysics, Chinese Academy of Science, Beijing 100101, China

Supporting Information

ABSTRACT: Cyanohydrin derivatives as enterovirus 71 (EV71) 3C protease ($3C^{pro}$) inhibitors have been synthesized and assayed for their biochemical and antiviral activities. Compared with the reported inhibitors, cyanohydrins (**1*S*,2*S*,2′*S*,5*S*)-16** and (**1*R*,2*S*,2′*S*,5*S*)-16** exhibited significantly improved activity and attractive selectivity profiles against other proteases, which were a result of the specific interactions between the cyanohydrin moiety and the catalytic site of $3C^{pro}$. Cyanohydrin as an anchoring group with high selectivity and excellent inhibitory activity represents a useful choice for cysteine protease inhibitors.

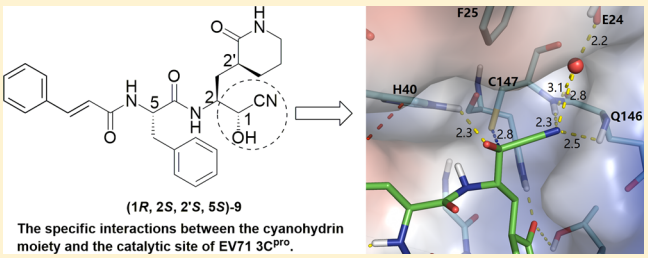

INTRODUCTION

Cysteine proteases are an important class of enzymes that are heavily involved in various human physiological processes.[1] Functional abnormalities of cysteine proteases may lead to human diseases, for instance, inflammatory diseases, neurodegenerative disorders, rheumatoid arthritis, and Alzheimer's disease, among others.[2] Thus, cysteine proteases are an attractive class of targets for drug discovery. Many inhibitors have been discovered and developed, for example, belnacasan as a caspase-1 inhibitor for the treatment of interleukin-1β converting enzyme-related diseases.[3] Peptidomimetic approaches have been widely adopted in drug discovery targeting cysteine proteases. On the basis of the peptide substrate cleavage specificity of the proteases, peptidomimetic inhibitors generally share a common structure: (1) a modified peptide recognition sequence for specific binding to the protease and (2) a C-terminal electrophilic functional group for anchoring the active-site cysteine.[1] On the basis of the characterization of the binding modes, the inhibitors can be broadly divided into the reversibles (e.g., aldehydes, nitriles, α-keto amides, etc.) and the irreversibles (e.g., α, β-unsaturated esters, disulfides, etc.).[1] According to the mechanism of the interaction, the activity of the inhibitors is proportional to the electrophilicity of the reactive group. However, the covalent-irreversible modifiers have seen limited use as potential drug candidates because the strong reactive electrophiles are generally accompanied by poor selectivity toward other proteases[1] and potential toxicity caused by the formation of protein adducts.[4] Therefore, the important issue for cysteine protease inhibitors is the development of a highly selective functional group that can interact noncovalently with the cysteine residue. Cyanohydrin is scarcely reported as an anchoring group of cysteine protease inhibitors,[5] and cyanohydrins as human EV71 $3C^{pro}$ inhibitors with high selectivity are introduced here.

Human EV71, one of the major pathogens of hand, foot, and mouth disease, has caused several large outbreaks in infants and children since 1997, mostly in the Asia-Pacific region. Unfortunately, there are currently no antiviral drugs or vaccines clinically available.[6] EV71 $3C^{pro}$, a virus-encoded cysteine protease, plays a key role in the process of virus replication. The single-stranded, positive-sense RNA genome encodes a large polyprotein precursor, which is subsequently cleaved into four structural proteins (VP1−VP4) and seven nonstructural proteins (2A−3D).[6] $3C^{pro}$ is indispensable for all EV71 polyprotein cleavage processes, with the exception of the cleavages of VP1/2A and 3C/3D by 2A protease.[6] Meanwhile, $3C^{pro}$ reportedly

Received: May 28, 2015
Published: November 16, 2015

DOI: 10.1021/acs.jmedchem.5b01013
J. Med. Chem. 2015, 58, 9414−9420

interferes with host cell function.[7] Therefore, the essential role of $3C^{pro}$ makes it an attractive target for anti-EV71 drug discovery. In this brief article, we introduce cyanohydrin as an anchoring group of cysteine protease inhibitors with high selectivity against human EV71 $3C^{pro}$.

RESULTS AND DISCUSSION

A literature survey of EV71 $3C^{pro}$ inhibitors revealed that, in addition to the good inhibition exhibited by rupintrivir (IC_{50} = 2.3 ± 0.5 μM),[8] derivative **1**[9] (IC_{50} < 0.5 μM, EC_{50} = 0.096 ± 0.006 μM) with aldehyde as an electrophile (Figure 1) possessed

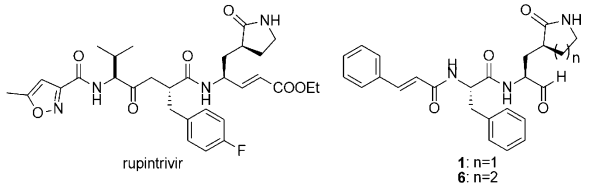

Figure 1. Structures of rupintrivir, **1** and **6**.

even better activity. The crystal structure of EV71 $3C^{pro}$[10] and the co-crystal structure of rupintrivir/EV71 $3C^{pro}$[8,11] revealed that, in the (*S*)-γ-lactam fragment, the carbonyl moiety forms a hydrogen bond with the imidazole segment of His161 and the amide nitrogen donates a hydrogen bond to the Thr142 backbone. Our research was initiated based on the hypothesis that the replacement of the (*S*)-γ-lactam ring by a (*S*)-δ-lactam ring could improve the potency against EV71 $3C^{pro}$. As shown in Figure 2, the (*S*)-δ-lactam ring displayed shorter hydrogen bond

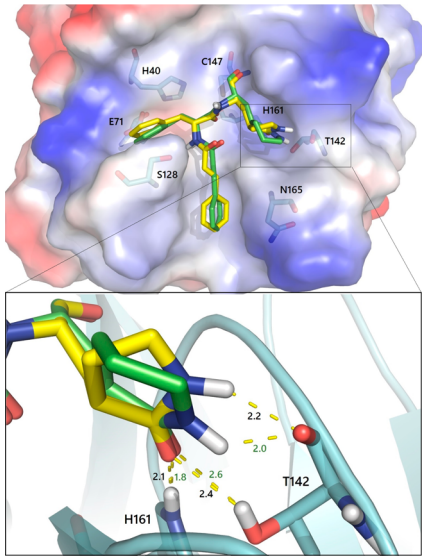

Figure 2. Comparison between the docking models of **1** (yellow) and **6** (green) bound to EV71 $3C^{pro}$.

distances and more preferable orientation than the (*S*)-γ-lactam ring when being docked into EV71 $3C^{pro}$. To validate our hypothesis, aldehyde **6** with a (*S*)-δ-lactam ring was synthesized together with aldehyde **1** as a reference (Scheme 2). The key intermediate **2** was prepared similarly to literature, and the stereochemistry and high diastereoselectivity were consistent with publications (see Scheme 1, Figure 1, and Part Q in Supporting Information (SI)).[9,12] Removal of the Boc group of **2** with TFA followed by an amide bond formation using EDCI as

Scheme 1. Representative Synthetic Scheme of Aldehyde 6

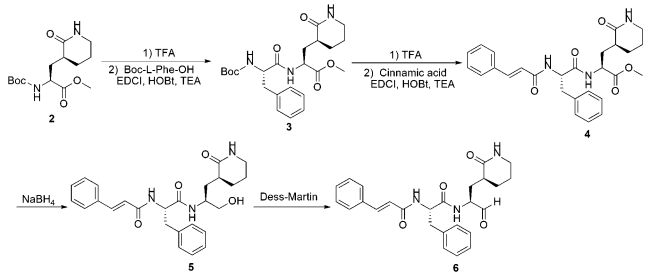

coupling reagent resulted in **3**, which was subsequently reacted with cinnamic acid to give **4** through a similar procedure. Alcohol **5**, obtained by the reduction of ester **4** with $NaBH_4$, was finally oxidized to aldehyde **6** with Dess–Martin periodinane. The biological activities (Table 1) indicated that **6** (IC_{50} = 0.54 ± 0.02 μM, EC_{50} = 0.26 ± 0.07 μM) presented approximately 7–10-fold

Table 1. Enzyme Inhibitory Activity, Antiviral Activity, and Cytotoxicity of 1, 5, 6, and 8–16 as EV71 $3C^{pro}$ Inhibitors

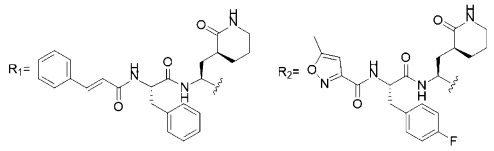

NO.		IC_{50}[a,b] (μM)	EC_{50}[b] (μM)	CC_{50}[b] (μM)
1	--	3.81 ± 0.19	3.07 ± 0.20	>100
6		0.54 ± 0.02	0.26 ± 0.07	>100
8		>10	>100	>100
11	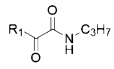	9.49 ± 1.11	4.59 ± 0.27	>100
9		1.13 ± 0.10	0.12 ± 0.05	>100
5		>10	>100	>100
14		>10	28.40 ± 1.33	>100
10	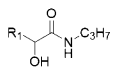	>10	>100	>100
12	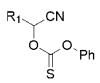	1.05 ± 0.09	0.15 ± 0.08	>100
13		1.62 ± 0.13	0.10 ± 0.06	>100
15		0.10 ± 0.02	0.11 ± 0.05	>100
16		0.28 ± 0.03	0.056 ± 0.004	>100
(**1S, 2S, 2′S, 5S**)-**16**		0.31 ± 0.03	0.045 ± 0.008	>100
(**1R, 2S, 2′S, 5S**)-**16**		0.27 ± 0.05	0.048 ± 0.006	>100

[a]The pH condition of biochemical assay for the inhibitors was 7.0 except (**1S,2S,2′S,5S**)-**16** and (**1R,2S,2′S,5S**)-**16** was 6.0. [b]Each data presents the average results from three independent experiments, and error bars represent SEMs (n = 3).

DOI: 10.1021/acs.jmedchem.5b01013
J. Med. Chem. 2015, 58, 9414–9420

better activities than **1** (IC_{50} = 3.81 ± 0.19 μM, EC_{50} = 3.07 ± 0.20 μM) in both the protease and cellular assays. The observed IC_{50} and EC_{50} values for **1** were different from the previously reported values[9] because of the use of different enzyme biochemical assays[13] and cell-based EV71 assays.[14] Additionally, the cellular activity is more potent than that of enzymatic activity, which is consistent with the observations in the published literatures about 3C and 3C-like protease inhibitors.[8,9,15] The enhanced efficacy and low toxicity of **6** (CC_{50} > 100 μM) directed our attention to the (*S*)-*δ*-lactam ring analogues.

Despite the significant improvement in biological activities, **6** as an aldehyde inhibitor may lead to various issues, such as low selectivity,[16] in further development. Therefore, we shifted our efforts to replace aldehyde with other anchoring functional groups. Nitriles are well-established cysteine protease inhibitors,[17] and α-keto amides possess good inhibition to calpain, which is a calcium-activated cysteine protease.[18] A series of compounds were synthesized (Scheme 2). The intermediate

Scheme 2. Synthetic Scheme of 8−14

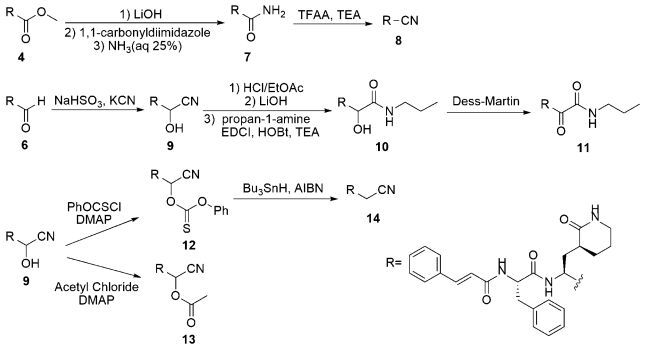

carboxylic acid was reacted with carbonyldiimidazole after the saponification of ester **4** with aqueous lithium hydroxide, and then the resulting imidazolide was quenched in situ with aqueous NH_3 to provide amide **7**. Amide **7** was converted to nitrile **8** by $(CF_3CO)_2O$-mediated dehydration.[19] Reaction of aldehyde **6** with KCN and $NaHSO_3$ afforded the corresponding cyanohydrin **9**.[20] Cyanohydrin **9** was then converted to the methyl ester with hydrochloric acid gas and ethyl acetate.[21] Then the carboxylic acid, derived from the hydrolysis of the intermediate methyl ester, coupled with amine to provide **10**. α-Keto amide **11** was the oxidative products of **10**. **14** was achieved in a two-step process via the reduction of the corresponding thionocarbonate ester derivative of **9**.[22] Ester **12** was the methyl ester derivative of **9**. The biological results showed that, nitrile **8** surprisingly exhibited no inhibitory activities (IC_{50} > 10 μM and EC_{50} > 100 μM) (Table 1). In addition, the anti-EV71 activities of α-keto amide **11** (IC_{50} = 9.49 ± 1.11 μM, EC_{50} = 4.59 ± 0.27 μM) presented greater than 10-fold activity loss compared to **6**. The further study of nitriles and α-keto amides was terminated due to the unsatisfactory biological activities.

To our surprise, compared to aldehyde **6**, cyanohydrin **9**, the synthetic precursor of α-keto amides, presented a relatively weak enzyme inhibitory activity (IC_{50} = 1.13 ± 0.1 μM) but greater than 2-fold enhancement in cellular activity with an EC_{50} of 0.12 ± 0.05 μM. To rapidly obtain more knowledge regarding the cyanohydrin group, we focused on the modifications of both −CN and −OH in the cyanohydrin group based on the epimeric mixture of cyanohydrins **9**. With the removal of −CN or −OH, the inhibitors exhibited a dramatic loss in efficacy against $3C^{pro}$, indicating that both −CN and −OH play critical roles in activity. The virus replication in virus-infected RD cells was attenuated by the treatment of **14** with an EC_{50} of 28.40 ± 1.33 μM, whereas **5** provided no inhibition, even at the highest concentration tested (EC_{50} > 100 μM). It was hypothesized that the nitrile group and the α-carbon in cyanohydrin contributed synergistically to the activity. Hence, further studies on −CN/−OH were performed. Following the replacement of −CN with an amide group, α-hydroxy amide **10** exhibited no activity against EV71 at the highest concentration tested (IC_{50} > 10 μM, EC_{50} > 100 μM). Moreover, with the esterification of −OH by a phenoxythiocarbonyl or acetyl group, derivatized cyanohydrins **12** (IC_{50} = 1.05 ± 0.09 μM, EC_{50} = 0.15 ± 0.08 μM) and **13** (IC_{50} = 1.62 ± 0.13 μM, EC_{50} = 0.10 ± 0.06 μM) presented nearly identical efficacy as **9** against $3C^{pro}$ and EV71 viral replication. These findings suggested that the presence of the −CN group and the electrophilicity of the α-carbon play important roles in the process of cyanohydrin binding to EV71 $3C^{pro}$.

In parallel to the structure−activity relationship study, the X-ray crystal structure study resulted in elucidation of the cocrystal structure of (**1*R***, **2*S***, **2′*S***, **5*S***)-**9**/EV71 $3C^{pro}$, which was determined at a 2.7 Å resolution during the crystallization experiment of the epimeric mixture of cyanohydrins **9** with EV71 $3C^{pro}$ (Protein Data Bank code 5BPE). The binding mode is presented in Figure 3 with the electrostatic potential mapped on

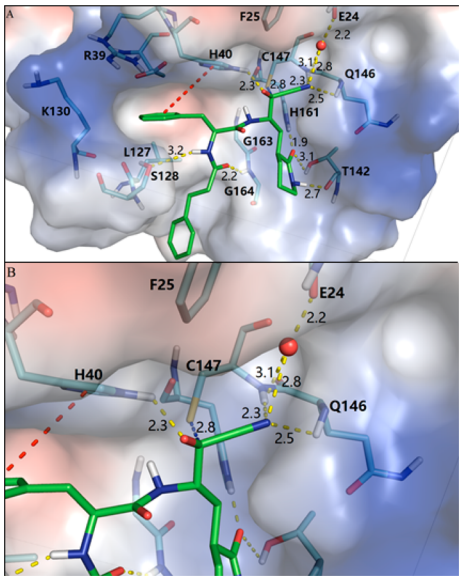

Figure 3. (A) X-ray co-crystal structure of (**1*R*,2*S*,2′*S*,5*S***)-**9**/EV71 $3C^{pro}$. (B) Partial enlargement for (**1*R*,2*S*,2′*S*,5*S***)-**9**/EV71 $3C^{pro}$ complex at S1′ pocket.

the solvent-accessible surface of $3C^{pro}$. The most important interactions between (**1*R*,2*S*,2′*S*,5*S***)-**9** and $3C^{pro}$ are highlighted in this figure. Similar to the rupintrivir-liganded protease complex,[8] the overall structure of the (**1*R*,2*S*,2′*S*,5*S***)-**9**-bound form of EV71 $3C^{pro}$ adopts the typical chymotrypsin-like fold. The S_1 pocket is formed by Thr142, His161, Gly163, and Gly164. The (*S*)-*δ*-lactam ring engages in two intermolecular hydrogen-bonding interactions with the side chain and the backbone of Thr142 as donors with distances of 3.1 and 2.7 Å, respectively. Additionally, the NH proton of His161 forms a hydrogen bond (1.9 Å), with the lone pair supplied by the (*S*)-*δ*-lactam ring oxygen. The larger S_2 pocket is able to accommodate the more deeply sunk P_2 fragment. Arg39 is located at the back of

DOI: 10.1021/acs.jmedchem.5b01013
J. Med. Chem. 2015, 58, 9414−9420

the S_2 pocket, forming a $\pi-\pi$ stacking interaction with the P_2 benzene ring. The P_3 phenylethylene group occupies the S_3 pocket, with its phenyl ring extending vertically along the binding groove. The cyanohydrin occupies the S_1' pocket and is in close proximity to the protease catalytic center. Compared to α,β-unsaturated ethyl ester in rupintrivir, one of striking differences is that the cyanohydrin moiety of (**1***R*,**2***S*,**2′***S*,**5***S*)-**9** interacts with Cys147. Neither −CN nor −OH form a hydrogen bond with the thiol of Cys147. However, because of the electron-withdrawing profile of −OH and −CN, the α-carbon of cyanohydrin exhibits electrophilicity to a certain extent, which forms a noncovalent interaction (2.8 Å) with the thiol (Figure 3B). This specific binding element is critical for the cyanohydrin function. Furthermore, the −CN of cyanohydrin participates in a bridge with a tightly bound water molecule in the S_1' pocket to stabilize the binding of the inhibitor−protein complex, and the nitrogen is within hydrogen-bonding distances of 2.5 and 2.3 Å to the backbones of Gln146 and Cys147, respectively. The −OH of cyanohydrin interacts with His40 (2.3 Å) as a hydrogen bond acceptor. Kinetic measurements were also performed. The inhibition of EV71 $3C^{pro}$ by **9** was independent of incubation time and competitive, with a K_i of 0.77 μM (see Part C in SI). These observations were consistent with a reversible, noncovalent mechanism of inhibition.

Further optimization of **9** led to the discovery of cyanohydrin **16**, which contained the P_2 *para*-fluorine benzyl group and P_3 5-methylisoxazole fragment (Scheme 3). The docking models of

Scheme 3. Synthetic Scheme of 16

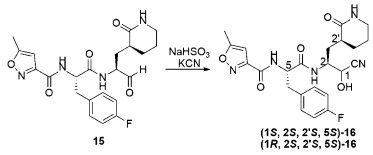

(**1***S*,**2***S*,**2′***S*,**5***S*)-**16** and (**1***R*,**2***S*,**2′***S*,**5***S*)-**16** bound to EV71 $3C^{pro}$ (Figure 4) indicated that the introduction of *para*-fluoro benzyl

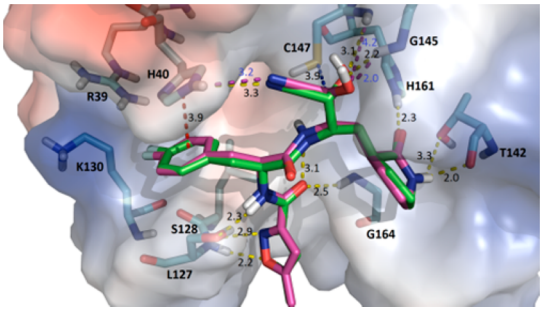

Figure 4. Comparison between the docking models of (**1***S*,**2***S*,**2′***S*,**5***S*)-**16** (purple) and (**1***R*,**2***S*,**2′***S*,**5***S*)-**16** (green) bound to EV71 $3C^{pro}$.

influences the electron distribution of the S_2 pocket, thus enhancing the interaction with positively charged Arg39. Additionally, the P3-isoxazole could form hydrogen interactions with surrounding residues (Ser128, Leu127) of $3C^{pro}$. There is an intramolecular hydrogen bond formed between the atoms on the skeleton structure. Indeed, as shown in Table 1, the epimeric mixture of cyanohydrins **16** exhibited better inhibition against EV71 $3C^{pro}$ (IC_{50} = 0.28 ± 0.03 μM) than that of **9**, which was consistent with **15**[23] (IC_{50} = 0.10 ± 0.02 μM) that had more than 5-fold improved inhibitory activity than that of **6**. We next separated the epimeric mixture of cyanohydrins **16** to (**1***S*,**2***S*,**2′***S*,**5***S*)-**16** and (**1***R*,**2***S*,**2′***S*,**5***S*)-**16**. The absolute configuration of the chiral carbon of cyanohydrin was determined by modified Mosher's method[24] and further supported by ^{1}H NMR and the calculated results of energy minimization by MOE (see Part B in SI). Epimerization of the chiral carbon of cyanohydrin only occurred at pH > 6.0 in Tris-HCl buffer, while no epimerization was observed at pH ≤ 6.0 in buffer and other solvents (see Figures 20−23 in SI). To obtain the enzyme inhibitory activity of the pure isomers (**1***S*,**2***S*,**2′***S*,**5***S*)-**16** and (**1***R*,**2***S*,**2′***S*,**5***S*)-**16**, the pH condition of biochemical assay was adjusted to 6.0, in which there should be no cyanohydrin epimerization (see Figure 24 in SI) and little impact was observed with the assay. Interestingly, (**1***S*,**2***S*,**2′***S*,**5***S*)-**16** and (**1***R*,**2***S*,**2′***S*,**5***S*)-**16** exhibited similar activities in protease and cellular assays. The interactions of (**1***S*,**2***S*,**2′***S*,**5***S*)-**16**/(**1***R*,**2***S*,**2′***S*,**5***S*)-**16** docked to EV71 $3C^{pro}$ could help to explain their unsubstantial difference in IC_{50} values (0.31 ± 0.03 vs 0.27 ± 0.05 μM). As illustrated in Figure 4, in addition to the noncovalent bond between the α-carbon and the thiol in the S_1' pocket, (**1***S*,**2***S*,**2′***S*,**5***S*)-**16** and (**1***R*,**2***S*,**2′***S*,**5***S*)-**16** have almost the same interactive distances between the nitrogen of −CN and His40. Moreover, the corresponding distances between −OH and Gly145/Cys147 are 2.0 and 4.2 Å in the (**1***S*,**2***S*,**2′***S*,**5***S*)-**16** model, respectively, compared to 2.2 and 3.1 Å in the (**1***R*,**2***S*,**2′***S*,**5***S*)-**16** model. However, although aldehyde **15** presented a strong enzyme inhibitory potency compared to the corresponding cyanohydrin **16**, improved antiviral activity of **16** was observed in the cellular assay. The calculated log *P* value of **16** (0.54) is 1.5-fold higher than that of aldehyde **15** (0.34). This could be the main factor that the cyanohydrin **16** could have better cellular penetration compared with the aldehyde **15** (EC_{50} = 0.11 ± 0.05 μM). Further, aldehyde as a reactive functional group could react with various nuleophiles in the cell. Therefore, the aldehyde may be consumed by nucleophile in the cell that results in less exposure. In addition, the epimeric mixture of cyanohydrins **16** (EC_{50} = 0.056 ± 0.004 μM), (**1***S*,**2***S*,**2′***S*,**5***S*)-**16** (EC_{50} = 0.045 ± 0.008 μM), and (**1***R*,**2***S*,**2′***S*,**5***S*)-**16** (EC_{50} = 0.048 ± 0.006 μM) exhibited equipotent antiviral activities in the cell-based assay. Compared with the reported inhibitor **1** with an aldehyde group (EC_{50} = 3.07 ± 0.20 μM), cyanohydrin derivatives (**1***S*,**2***S*,**2′***S*,**5***S*)-**16**/(**1***R*,**2***S*,**2′***S*,**5***S*)-**16** exhibited more than 80-fold higher antiviral activities. Additionally, favorable CC_{50} values (CC_{50} > 100 μM) were observed for all of the inhibitors in the in vitro cytotoxicity assay.

Cyanohydrin derivatives are present in a number of natural products such as mandelonitrile,[25] cyanohydrin phosphonate,[26] and α-ketoglutarate cyanohydrin (α-kgCN) in animals.[27] More importantly, cyanohydrin derivatives have been used as prescription drugs for treating asthma and proved to possess high potential in cancer chemotherapy.[28,29] Because cyanogenic glycosides can potentially degrade into hydrogen cyanide in a process known as cyanogenesis,[30] we focused more attention on the toxicity of the cyanohydrin derivative as an EV71 $3C^{pro}$ inhibitor. Compared to a LD_{50} of 2.6 mg/kg for KCN[31] in mice via intravenous injection, the acute toxicokinetic behavior of (**1***R*,**2***S*,**2′***S*,**5***S*)-**16** represented tolerated toxicity with a LD_{50} of 96.5 mg/kg.

Selectivity is one of the general issues for protease inhibitors, particularly those with reactive electrophiles such as aldehyde. We profiled selected inhibitors containing either cyanohydrin or aldehyde while keeping the rest of the structure constant against a list of proteases available to our research group. The inhibition

DOI: 10.1021/acs.jmedchem.5b01013
J. Med. Chem. 2015, 58, 9414−9420

ratios of **15**, (**1***S*,**2***S*,**2′***S*,**5***S*)-**16**, and (**1***R*,**2***S*,**2′***S*,**5***S*)-**16** were determined against serine protease (human neutrophil elastase (HNE), human trypsin (*h*Trypsin), human chymotrypsin (*h*chymotrypsin), porcine pancreatic elastase (PPE), acetylcholine esterase (AChE) and butyrylcholinesterase (BChE)) and cysteine protease (EV71 3C^{pro} and severe acute respiratory syndrome coronaviruses main protease (SARS CoV M^{pro})).[32] As indicated by the results summarized in Figure 5, in contrast to the

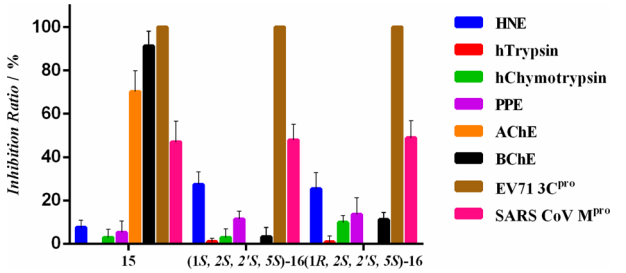

Figure 5. **15**, (**1***S*,**2***S*,**2′***S*,**5***S*)-**16** and (**1***R*,**2***S*,**2′***S*,**5***S*)-**16** (100 μM) protease inhibitory activities of HNE, *h*Trypsin, *h*Chymotrypsin, PPE, AChE, BChE, EV71 3C^{pro}, and SARS CoV M^{pro}. Vertical bars represent the standard deviation of each data point (n = 3).

low selectivity of **15**, (**1***S*,**2***S*,**2′***S*,**5***S*)-**16** and (**1***R*,**2***S*,**2′***S*,**5***S*)-**16** both exhibited significantly high selectivities for EV71 3C^{pro} and SARS CoV M^{pro} over other proteases. The selectivities of (**1***S*,**2***S*,**2′***S*,**5***S*)-**16** and (**1***R*,**2***S*,**2′***S*,**5***S*)-**16** are presumably related to the specificity of the cyanohydrin. Therefore, cyanohydrin potentially represents a good choice as an anchoring group for cysteine protease inhibitors because of its high selectivity and good inhibitory activity.

CONCLUSIONS

In conclusion, cyanohydrin derivatives as potent inhibitors of EV71 3C^{pro} have been described. The cocrystal structure of cyanohydrin inhibitor and 3C^{pro} was resolved, and the interactions between the cyanohydrin group and 3C^{pro} were revealed. On the basis of the data analysis of the co-crystal structure, a number of potent EV71 3C^{pro} inhibitors were discovered, and the antiviral efficacies of the inhibitors were significantly improved. Importantly, cyanohydrin as an anchoring group with high selectivity and excellent inhibitory activity provides a useful choice for cysteine protease inhibitors.

EXPERIMENTAL SECTION

General. All reagents were purchased from commercial suppliers and used as received. NMR spectra were recorded on a Bruker AVANCE-400 (400 MHz) (Bruker, Karlsruhe, Germany) NMR spectrometer. Molecular mass was determined by ESI mass spectrometry using a Shimadzu LCMS-2020 (Shimadzu, Kyoto, Japan). Optical rotations were measured with an Insmark IP-120 automatic polarimeter (Insmark, Shanghai, China). Measurements were collected at 15 °C in DCM at 589 nm. $[\alpha]_D$ values are given in units of (deg × mL)/(g × dm). HRMS were recorded on a high-resolution ESI-FTICR mass spectrometer (Varian 7.0 T, Varian, USA). All tested compounds exhibited purities of >95% as analyzed by HPLC (Dionex UltiMate 3000, Germany).

*General Procedure for the Synthesis of Aldehydes (**1**, **6**, and **15**). Preparation of Aldehyde **6**.* To a solution of **5** (2.1 g, 4.7 mmol) in anhydrous DCM (30.0 mL) was added Dess−Martin reagent (3.0 g, 7.1 mmol) slowly at 0 °C. Then, the reaction mixture was stirred at RT for 1 h. A solution of $NaHCO_3$ and $Na_2S_2O_3$ was added to quench the reaction. After 10 min, DCM (30.0 mL × 2) was added to extract the mixture. The organic phase was washed with brine (30 mL × 2), dried over Na_2SO_4, and concentrated, and the residue was purified by column chromatography (DCM:MeOH, 35:1 v/v) to afford the pure product as a white solid **6** (1.70 g, 3.8 mmol, 81%); $[\alpha]_D^{15}$ = −2.4 (c = 0.21 g/100 mL, MeOH). ^{1}H NMR (400 MHz, $CDCl_3$) δ: 9.22 (s, 1H), 7.48 (d, J = 4.4 Hz, 2H), 7.42−7.17 (m, 9H), 6.47 (d, J = 15.6 Hz, 1H), 5.12−4.89 (m, 1H), 4.33−4.20 (m, 1H), 3.35 (d, J = 11.7 Hz, 1H), 3.31−3.17 (m, 3H), 2.23 (dt, J = 13.6, 6.8 Hz, 1H), 2.17−2.06 (m, 1H), 1.98 (s, 2H), 1.91−1.83 (m, 1H), 1.69 (dd, J = 20.0, 11.4 Hz, 1H), 1.59−1.45 (m, 1H). ^{13}C NMR (100 MHz, $CDCl_3$) δ: 200.15, 174.90, 171.91, 165.58, 141.57, 136.42, 134.69, 129.82, 129.70, 129.58, 129.53, 128.82, 128.60, 128.57, 127.88, 127.01, 120.31, 57.41, 54.27, 42.31, 38.82, 37.49, 30.79, 27.53, 21.30. HRMS (ESMS): $C_{26}H_{29}N_3NaO_4$ (M + Na)$^+$ calcd, 470.2050; found, 470.2052.

*Preparation of Nitrile **8**.* To a solution of **7** (1.77 g, 3.83 mmol) and Et_3N (1.33 mL, 9.58 mmol) in 100 mL of anhydrous THF, trifluoroacetic acid anhydride (TFAA) (0.97 g, 4.60 mmol) was added dropwise at −5 °C. The reaction mixture was stirred at 0 °C for 2 h and then partitioned between EtOAc and H_2O. The organic phase was dried over Na_2SO_4 and concentrated, and the residue was purified by column chromatography (DCM:MeOH, 35:1 v/v) to afford the pure product as a white solid **8** (1.51 g, 89%); $[\alpha]_D^{15}$ = −9.0 (c = 0.16, DCM). ^{1}H NMR (400 MHz, DMSO-d_6) δ: 7.55 (d, J = 7.0 Hz, 3H), 7.46−7.37 (m, 4H), 7.28 (d, J = 4.2 Hz, 4H), 6.70 (d, J = 15.8 Hz, 1H), 5.04 (dd, J = 15.6, 7.9 Hz, 1H), 4.59 (m, 1H), 3.06 (m, 3H), 2.87 (dd, J = 13.6, 9.5 Hz, 1H), 2.29−2.16 (m, 2H), 1.78 (m, 3H), 1.65−1.51 (m, 1H), 1.40 (m, 1H). ^{13}C NMR (100 MHz, DMSO-d_6) δ: 172.48, 171.75, 165.33, 139.58, 137.93, 135.23, 130.02, 129.59, 129.42, 128.64, 128.01, 126.91, 122.19, 119.96, 116.99, 54.67, 41.55, 39.08, 37.88, 37.34, 34.48, 26.55, 21.63. HRMS (ESMS): $C_{26}H_{28}N_4NaO_3$ (M + Na)$^+$ calcd, 467.2054; found, 467.2060.

*General Procedure for the Synthesis of Cyanohydrins (**9** and **16**): Preparation of Cyanohydrin **9**.* To a solution of **6** (500 mg, 1.1 mmol) in DCM (20 mL) was added saturated $NaHSO_3$ (149 mg, 1.4 mmol) solution. The mixture was stirred at RT for 0.5 h, and then an aq solution of KCN (86 mg, 1.3 mmol) was added. The mixture was stirred at RT for 12 h. Then, the organic phase was collected and the aqueous layer was extracted with DCM (30 mL × 3). The combined organic phase was washed with brine (30 mL × 2), dried over Na_2SO_4, and concentrated, and the residue was purified by column chromatography (DCM:MeOH, 33:1 v/v) to afford the pure product as a white solid **9** (480 mg, 1.01 mmol, 92%). ^{1}H NMR (400 MHz, $CDCl_3$) δ: 7.54 (d, J = 15.6 Hz, 1H), 7.49−7.38 (m, 2H), 7.36−7.15 (m, 8H), 6.43 (d, J = 4.7 Hz, 1H), 4.96 (dd, J = 13.9, 6.8 Hz, 1H), 4.57−4.46 (m, 1H), 4.23 (dd, J = 12.6, 9.2 Hz, 1H), 3.29−3.05 (m, 4H), 2.24 (m, 2H), 2.03−1.90 (m, 1H), 1.86−1.70 (m, 2H), 1.65 (dd, J = 12.8, 5.3 Hz, 1H), 1.44 (dd, J = 22.0, 11.3 Hz, 1H). ^{13}C NMR (100 MHz, $CDCl_3$) δ: 175.42, 172.86, 166.07, 141.67, 136.36, 134.62, 129.83, 129.48, 128.80, 128.58, 127.92, 126.99, 120.23, 118.72, 64.30, 54.57, 51.25, 42.25, 38.47, 31.50, 26.99, 21.15. HRMS (ESMS): $C_{27}H_{30}N_4NaO_4$ (M + Na)$^+$ calcd, 497.2159; found, 497.2158.

*Cyanohydrin **16**.* **16** (94% yield) was purified by column chromatography (DCM: MeOH, 33:1 v/v) to afford the two pure products as white solids: (**1***S*,**2***S*,**2′***S*,**5***S*)-**16**; 44% yield; $[\alpha]_D^{28}$ = −160.04 (c = 0.031 g/100 mL, DCM). ^{1}H NMR (400 MHz, $CDCl_3$) δ: 8.60 (d, J = 6.8 Hz, 1H), 7.60 (d, J = 8.1 Hz, 1H), 7.21 (dd, J = 7.7, 5.7 Hz, 2H), 6.96 (t, J = 8.5 Hz, 2H), 6.37 (s, 1H), 4.92 (q, J = 14.0, 7.1 Hz, 1H), 4.54 (d, J = 2.9 Hz, 1H), 4.20 (m, 1H), 3.30 (m, 2H), 3.23 (dd, J = 14.0, 5.8 Hz, 1H), 3.13 (dd, J = 14.0, 7.3 Hz, 1H), 2.46 (s, 3H), 2.28 (tt, J = 10.4, 5.1 Hz, 2H), 2.02 (dd, J = 8.4, 4.0 Hz, 1H), 1.87 (dd, J = 9.5, 4.1 Hz, 1H), 1.79−1.62 (m, 2H), 1.54 (dd, J = 22.2, 11.0 Hz, 1H). ^{13}C NMR (100 MHz, $CDCl_3$) δ: 175.38, 172.32, 171.38, 161.97 (d, J_{C-F} = 245.2 Hz), 159.18, 158.14, 131.81 (d, J_{C-F} = 3.0 Hz), 130.99 (d, J_{C-F} = 7.9 Hz), 118.26, 115.46 (d, J_{C-F} = 21.2 Hz), 101.38, 65.06, 54.46, 52.22, 42.29, 37.89, 37.52, 31.31, 27.26, 21.27, 12.31. HRMS (ESMS): $C_{23}H_{26}FN_5NaO_5$ (M + Na)$^+$ calcd, 494.1810; found, 494.1815. (**1***R*,**2***S*,**2′***S*,**5***S*)-**16**: 50% yield; $[\alpha]_D^{28}$ = −41.88 (c = 0.028 g/100 mL, DCM). ^{1}H NMR (400 MHz, $CDCl_3$) δ: 8.38 (d, J = 7.4 Hz, 1H), 7.61 (d, J = 8.1 Hz, 1H), 7.23 (d, J = 7.2 Hz, 2H), 6.96 (t, J = 8.2 Hz, 2H), 6.35 (s, 1H), 4.93 (q, J = 14.1, 7.0 Hz, 1H), 4.57 (d, J = 4.3 Hz, 1H), 4.24 (m, 1H), 3.36−3.17 (m, 3H), 3.12 (dd, J = 14.0, 7.5 Hz, 1H), 3.29 (m, 2H), 3.22 (dd, J = 13.7, 7.8 Hz, 1H), 3.12 (dd, J = 14.0, 7.5 Hz, 1H), 2.46 (s, 3H), 2.36−2.14 (m, 2H), 2.10−1.97 (m, 1H), 1.77 (m, 3H), 1.51 (dd, J

DOI: 10.1021/acs.jmedchem.5b01013
J. Med. Chem. 2015, 58, 9414−9420

= 21.8, 10.7 Hz, 1H). ^{13}C NMR (100 MHz, $CDCl_3$) δ: 175.56, 172.00, 171.32, 161.96 (d, J_{C-F} = 245.0 Hz), 159.10, 158.18, 131.86 (d, J_{C-F} = 3.1 Hz), 131.01 (d, J_{C-F} = 8.0 Hz), 118.62, 115.45 (d, J_{C-F} = 21.3 Hz), 101.38, 64.19, 54.51, 51.25, 42.31, 37.72, 37.64, 31.43, 26.95, 21.19, 12.30. HRMS (ESMS): $C_{23}H_{26}FN_5NaO_5$ $(M + Na)^+$ calcd, 494.1810; found, 494.1812.

Preparation of α-Hydroxy Amide ***10***. **9** (379 mg, 0.80 mmol) was dissolved in a solution of 4 N HCl/EtOAc (4 mL) and MeOH (4 mL), and the mixture was refluxed for 16 h under a N2 atm. After concentrating, the residue was dissolved in DCM, washed with brine (30 mL × 2), dried over Na_2SO_4, and concentrated. The obtained residue was dissolved in MeOH:H_2O (150 mL, 25:3 v/v) at RT, and then LiOH (28.8 mg, 1.2 mmol) was added. After 1.5 h, the pH of the reaction mixture was adjusted to 3.0. The mixture was extracted with EtOAc (100 mL × 3), and the organic phase was dried over Na_2SO_4 and concentrated to afford the pure product as a white solid intermediate, which was engaged in an amide bond formation with propan-1-amine (56.74 mg, 0.96 mmol) to afford a white solid **10** (353 mg, 0.68 mmol, 85% yield). ^{1}H NMR (400 MHz, $CDCl_3$) δ: 7.54 (d, J = 15.7 Hz, 1H), 7.44−7.38 (m, 2H), 7.30 (dd, J = 5.1, 1.4 Hz, 3H), 7.20−7.06 (m, 3H), 6.91 (t, J = 8.6 Hz, 2H), 6.53 (d, J = 15.7 Hz, 1H), 5.44 (s, 1H), 4.95 (dd, J = 14.0, 6.4 Hz, 1H), 4.36−4.26 (m, 1H), 3.16 (m, 4H), 2.46−2.18 (m, 1H), 2.10−1.98 (m, 1H), 1.98−1.86 (m, 1H), 1.71 (dd, J = 8.7, 4.0 Hz, 1H), 1.64−1.32 (m, 6H), 1.26 (s, 1H), 0.88 (t, J = 7.4 Hz, 3H). ^{13}C NMR (100 MHz, $CDCl_3$) δ: 175.71, 172.22, 171.35, 166.03, 141.40, 134.64, 132.54, 131.06, 130.98, 129.82, 128.81, 127.88, 120.45, 115.34, 115.13, 74.20, 54.66, 53.46, 52.16, 42.31, 40.78, 38.11, 37.40, 30.75, 29.71, 27.21, 22.80, 21.14, 11.40. HRMS (ESMS): $C_{30}H_{38}N_3O_5$ $(M + H)^+$ calcd, 520.2806; found, 520.2810.

α-Keto Amide ***11***. $[\alpha]_D^{15}$ = −40.8 (c = 0.08 g/100 mL, DCM). ^{1}H NMR (400 MHz, $CDCl_3$) δ: 7.58 (d, J = 15.6 Hz, 1H), 7.46 (dd, J = 6.3, 2.7 Hz, 2H), 7.39−7.31 (m, 3H), 7.19 (dd, J = 8.3, 5.5 Hz, 2H), 7.05 (t, J = 5.9 Hz, 1H), 6.94 (t, J = 8.6 Hz, 2H), 6.39 (d, J = 15.6 Hz, 1H), 5.29−5.22 (m, 1H), 5.03 (dd, J = 14.0, 6.1 Hz, 1H), 3.31−3.24 (m, 3H), 3.14 (t, J = 6.5 Hz, 1H), 2.29 (m, 1H), 2.17−1.97 (m, 3H), 1.93−1.83 (m, 1H), 1.79−1.68 (m, 1H), 1.64−1.50 (m, 3H), 1.25 (s, 2H), 0.94 (t, J = 7.4 Hz, 3H). ^{13}C NMR (100 MHz, $CDCl_3$) δ: 195.03, 175.00, 171.03, 165.43, 159.49, 141.54, 134.65, 132.14, 131.24, 131.16, 129.83, 128.83, 127.88, 120.24, 53.81, 53.57, 42.35, 38.57, 37.95, 32.62, 22.51, 21.59, 11.37. HRMS (ESMS): $C_{30}H_{35}N_3NaO_5$ $(M + Na)^+$ calcd, 540.2469; found, 540.2461.

*General Procedure for the Synthesis of Derivatized Cyanohydrins (***12** *and* **13***): Preparation of Derivatized Cyanohydrin* ***12***. To a solution of **9** (237 mg, 0.5 mmol) in DCM (30 mL) was added DMAP (488.68 mg, 4.0 mmol) and phenyl chlorothionoformate (345.26 mg, 2.0 mmol) under a N_2 atmosphere at 0 °C. The reaction mixture was stirred at RT for 2 h, poured into water, and extracted with DCM. The organic phase was washed with H_2O, dried over Na_2SO_4, and concentrated, and the residue was purified by column chromatography (DCM:MeOH, 50:1 v/v) to afford the pure product as a yellow solid **12** (289.8 mg, 0.48 mmol, 95%). ^{1}H NMR (400 MHz, $CDCl_3$) δ: 7.59 (d, J = 15.6 Hz, 1H), 7.44 (dd, J = 10.9, 4.3 Hz, 4H), 7.34 (dd, J = 8.1, 5.5 Hz, 5H), 7.31−7.28 (m, 3H), 7.13 (d, J = 7.8 Hz, 2H), 7.00 (d, J = 8.1 Hz, 1H), 6.50 (d, J = 15.7 Hz, 1H), 5.77 (d, J = 4.7 Hz, 1H), 5.18 (dd, J = 14.3, 6.7 Hz, 1H), 4.56−4.42 (m, 1H), 3.23 (tt, J = 13.7, 6.7 Hz, 4H), 2.60 (td, J = 13.8, 3.2 Hz, 1H), 2.34 (t, J = 13.6 Hz, 1H), 2.10−1.97 (m, 1H), 1.93−1.77 (m, 2H), 1.77−1.62 (m, 1H), 1.59−1.45 (m, 1H). ^{13}C NMR (100 MHz, $CDCl_3$) δ: 192.60, 174.49, 172.72, 165.66, 153.41, 141.48, 136.37, 134.70, 129.81, 129.46, 128.83, 128.72, 127.90, 127.15, 127.10, 121.63, 120.39, 114.25, 71.08, 54.36, 48.60, 42.18, 38.96, 37.56, 31.14, 26.98, 21.42. HRMS (ESMS): $C_{34}H_{34}N_4NaO_5S$ $(M + Na)^+$ calcd, 633.2142; found, 633.2148.

Preparation of Acetonitrile ***14***. To a solution of **12** (134 mg, 0.22 mmol) in toluene (40 mL) was added *tri-n*-butyltinhydride (223.3 mg, 0.77 mmol) and a catalytic amount of 2,2′-azobis(2-methylpropionitrile) under a N_2 atmosphere. The reaction mixture was stirred under reflux for 1 h, cooled, and concentrated. The residue was purified by column chromatography (DCM:MeOH, 20:1 v/v) to afford the pure product as a white solid **14** (71.6 mg, 0.16 mmol, 71%); $[\alpha]_D^{15}$ = −15.7 (c = 0.15 g/100 mL, DCM). ^{1}H NMR (400 MHz, $CDCl_3$) δ: 7.49 (d, J = 15.6 Hz, 1H), 7.38 (dd, J = 6.2, 2.6 Hz, 2H), 7.29−7.23 (m, 3H), 7.21−7.17 (m, 2H), 7.15 (t, J = 7.7 Hz, 3H), 6.39 (d, J = 15.6 Hz, 1H), 5.01 (dd, J = 14.8, 6.9 Hz, 1H), 3.94 (m, 1H), 3.18 (s, 2H), 3.05 (m, 2H), 2.48 (dd, J = 16.6, 4.0 Hz, 1H), 2.23−2.12 (m, 2H), 2.12−2.04 (m, 1H), 1.95−1.82 (m, 1H), 1.80−1.67 (m, 1H), 1.66−1.47 (m, 2H), 1.36 (m, 1H). ^{13}C NMR (100 MHz, $CDCl_3$) δ: 174.65, 171.82, 165.52, 141.45, 136.50, 134.69, 129.83, 129.53, 128.85, 128.53, 127.87, 126.99, 120.45, 117.40, 54.07, 44.83, 42.19, 39.15, 37.94, 34.87, 27.13, 23.51, 21.52. HRMS (ESMS): $C_{27}H_{30}N_4NaO_3$ $(M + Na)^+$ calcd, 481.2210; found, 481.2214.

*X-ray Co-crystal Structure of EV71 3C^{pro} Complexed with (1R, 2S, 2′S, 5S)-***9***.* The inhibitor (**1*R*,2*S*,2′*S*,5*S***)-**9** was mixed with EV71 3C^{pro} at a molar ratio of 5:1, and the optimal crystallization of EV71 3C^{pro} was achieved by mixing 1.0 μL of protein with 1.0 μL of buffer containing 100 mM Tris-HCl (pH 7.7), 200 mM sodium citrate, and 20% polyethylene glycol 3350 in a hanging-drop vapor diffusion system at 22 °C. Crystals appeared and reached their final size within 5 days. The resulting crystals were soaked in reservoir solution containing 15% ethylene glycol as the cryoprotectant and flash-frozen in liquid nitrogen. The native data set of EV71 3C^{pro} in complex with inhibitor was collected to 2.7 Å resolution at beamline BL17U of the Shanghai Synchrotron Radiation Facility (SSRF) with a wavelength of 0.9789 Å. The data were processed and scaled using the HKL2000 package.[33] The space group was identified as $C2$, and one molecule was found per asymmetric unit. The complex structure was determined using PHENIX[34] with the crystal structure of EV71 3C^{pro} (PDB code: 3OSY) as the initial searching model. Manual model construction and refinement were performed using COOT[35] and PHENIX following rigid body refinement, energy minimization, and individual B-factor refinement. The quality of the final refined model was verified using the program PROCHECK.[36] Data collection and the final model statistics are summarized in Table S1 of the SI.

■ ASSOCIATED CONTENT

Supporting Information

The Supporting Information is available free of charge on the ACS Publications website at DOI: 10.1021/acs.jmedchem.5b01013.

Detailed synthetic procedures, compound characterization, crystallographic data, and biochemical and antiviral assays (PDF)

Molecular formula strings (CSV)

■ AUTHOR INFORMATION

Corresponding Authors

*For Z.Y.: e-mail, zheng_yin@nankai.edu.cn.

*For L.S.: e-mail, shanglq@nankai.edu.cn.

Notes

The authors declare no competing financial interest.

■ ACKNOWLEDGMENTS

We thank the staff of SSRF BL17U1 for their support in collecting the diffraction data. This work was supported by the National Basic Research Program of China (973 program, grant nos. 2013CB911104, 2013CB911100), the National Natural Science Foundation of China (grant nos. 21202087, 81322023, 31170678, 31370733), the Tianjin Science and Technology Program (grant nos. 13JCYBJC24300, 13JCQNJC13100), and the "111" Project of the Ministry of Education of China (project no. B06005).

■ REFERENCES

(1) Otto, H. H.; Schirmeister, T. Cysteine Proteases and Their Inhibitors. *Chem. Rev.* **1997**, *97*, 133−171.

DOI: 10.1021/acs.jmedchem.5b01013
J. Med. Chem. 2015, 58, 9414−9420

(2) Leung-Toung, R.; Li, W. R.; Tam, T. F.; Kaarimian, K. Thiol-Dependent Enzymes and Their Inhibitors: A Review. *Curr. Med. Chem.* **2002**, *9* (9), 979−1002.
(3) (a) Leung, D.; Abbenante, G.; Fairlie, D. P. Protease Inhibitors: Current Status and Future Prospects. *J. Med. Chem.* **2000**, *43* (3), 305−341. (b) Abbenante, G.; Fairlie, D. P. Protease Inhibitors in the Clinic. *Med. Chem.* **2005**, *1* (1), 71−104.
(4) Shah, F.; Mukherjee, P.; Gut, J.; Legac, J.; Rosenthal, P. J.; Tekwani, B. L.; Avery, M. A. Identification of Novel Malarial Cysteine Protease Inhibitors Using Structure-Based Virtual Screening of a Focused Cysteine Protease Inhibitor Library. *J. Chem. Inf. Model.* **2011**, *51* (4), 852−864.
(5) Mehrtens, J. M. *The Design, Synthesis and Biological Assay of Cysteine Protease Specific Inbibitors*; University of Canterbury: Christchurch, New Zealand, 2007.
(6) Shang, L. Q.; Xu, M. Y.; Yin, Z. Antiviral Drug Discovery for the Treatment of Enterovirus 71 Infections. *Antiviral Res.* **2013**, *97* (2), 183−194.
(7) Weng, K. F.; Li, M. L.; Hung, C. T.; Shih, S. R. Enterovirus 71 3c Protease Cleaves a Novel Target Cstf-64 and Inhibits Cellular Polyadenylation. *PLoS Pathog.* **2009**, *5* (9), e1000593.
(8) Wang, J.; Fan, T. T.; Yao, X.; Wu, Z. Q.; Guo, L.; Lei, X. B.; Wang, J. W.; Wang, M. T.; Jin, Q.; Cui, S. Crystal Structures of Enterovirus 71 3c Protease Complexed with Rupintrivir Reveal the Roles of Catalytically Important Residues. *J. Virol.* **2011**, *85* (19), 10021−10030.
(9) Kuo, C. J.; Shie, J. J.; Fang, J. M.; Yen, G. R.; Hsu, J. T. A.; Liu, H. G.; Tseng, S. N.; Chang, S. C.; Lee, C. Y.; Shih, S. R.; Liang, P. H. Design, Synthesis, and Evaluation of 3c Protease Inhibitors as Anti-Enterovirus 71 Agents. *Bioorg. Med. Chem.* **2008**, *16* (15), 7388−7398.
(10) Cui, S.; Wang, J.; Fan, T. T.; Qin, B.; Guo, L.; Lei, X. B.; Wang, J. W.; Wang, M. T.; Jin, Q. Crystal Structure of Human Enterovirus 71 3c Protease. *J. Mol. Biol.* **2011**, *408* (3), 449−461.
(11) Wu, C. M.; Cai, Q. X.; Chen, C.; Li, N.; Peng, X. J.; Cai, Y. X.; Yin, K.; Chen, X. S.; Wang, X. L.; Zhang, R. F.; Liu, L. J.; Chen, S. H.; Li, J.; Lin, T. W. Structures of Enterovirus 71 3c Proteinase (Strain E2004104-Tw-Cdc) and Its Complex with Rupintrivir. *Acta Crystallogr., Sect. D: Biol. Crystallogr.* **2013**, *69*, 866−871.
(12) (a) Gu, Z. Q.; Hesson, D. P.; Pelletier, J. C.; Maccecchini, M. L.; Zhou, L. M.; Skolnick, P. Synthesis, Resolution, and Biological Evaluation of the 4 Stereoisomers of 4-Methylglutamic Acid - Selective Probes of Kainate Receptors. *J. Med. Chem.* **1995**, *38* (14), 2518−2520. (b) Hanessian, S.; Margarita, R. 1,3-Asymmetric Induction in Dianionic Allylation Reactions of Amino Acid Derivatives-Synthesis of Functionally Useful Enantiopure Glutamates, Pipecolates and Pyroglutamates. *Tetrahedron Lett.* **1998**, *39* (33), 5887−5890.
(13) Shang, L. Q.; Zhang, S. M.; Yang, X.; Sun, J. X.; Li, L. F.; Cui, Z. J.; He, Q. H.; Guo, Y.; Sun, Y. N.; Yin, Z. Biochemical Characterization of Recombinant Enterovirus 71 3c Protease with Fluorogenic Model Peptide Substrates and Development of a Biochemical Assay. *Antimicrob. Agents Chemother.* **2015**, *59* (4), 1827−1836.
(14) Shang, L. Q.; Wang, Y. X.; Qing, J.; Shu, B.; Cao, L.; Lou, Z. Y.; Gong, P.; Sun, Y. N.; Yin, Z. An Adenosine Nucleoside Analogue Nitd008 Inhibits Ev71 Proliferation. *Antiviral Res.* **2014**, *112*, 47−58.
(15) Prior, A. M.; Kim, Y. J.; Weerasekara, S.; Moroze, M.; Alliston, K. R.; Uy, R. A. Z.; Groutas, W. C.; Chang, K. O.; Hua, D. H. Design, Synthesis, and Bioevaluation of Viral 3c and 3c-Like Protease Inhibitors. *Bioorg. Med. Chem. Lett.* **2013**, *23* (23), 6317−6320.
(16) Rishton, G. M. Nonleadlikeness and Leadlikeness in Biochemical Screening. *Drug Discovery Today* **2003**, *8* (2), 86−96.
(17) Frizler, M.; Stirnberg, M.; Sisay, M. T.; Gutschow, M. Development of Nitrile-Based Peptidic Inhibitors of Cysteine Cathepsins. *Curr. Top. Med. Chem.* **2010**, *10* (3), 294−322.
(18) Harbeson, S. L.; Abelleira, S. M.; Akiyama, A.; Barrett, R.; Carroll, R. M.; Straub, J. A.; Tkacz, J. N.; Wu, C. C.; Musso, G. F. Stereospecific Synthesis of Peptidyl Alpha-Keto Amides as Inhibitors of Calpain. *J. Med. Chem.* **1994**, *37* (18), 2918−2929.
(19) Altmann, E.; Aichholz, R.; Betschart, C.; Buhl, T.; Green, J.; Irie, O.; Teno, N.; Lattmann, R.; Tintelnot-Blomley, M.; Missbach, M. 2-Cyano-Pyrimidines: A New Chemotype for Inhibitors of the Cysteine Protease Cathepsin K. *J. Med. Chem.* **2007**, *50* (4), 591−594.
(20) Malamas, M. S.; Erdei, J.; Gunawan, I.; Barnes, K.; Johnson, M.; Hui, Y.; Turner, J.; Hu, Y.; Wagner, E.; Fan, K.; Olland, A.; Bard, J.; Robichaud, A. J. Aminoimidazoles as Potent and Selective Human Beta-Secretase (Bace1) Inhibitors. *J. Med. Chem.* **2009**, *52* (20), 6314−6323.
(21) Ezzili, C.; Mileni, M.; McGlinchey, N.; Long, J. Z.; Kinsey, S. G.; Hochstatter, D. G.; Stevens, R. C.; Lichtman, A. H.; Cravatt, B. F.; Bilsky, E. J.; Boger, D. L. Reversible Competitive Alpha-Ketoheterocycle Inhibitors of Fatty Acid Amide Hydrolase Containing Additional Conformational Constraints in the Acyl Side Chain: Orally Active, Long-Acting Analgesics. *J. Med. Chem.* **2011**, *54* (8), 2805−2822.
(22) Palombo, E.; Audran, G.; Monti, H. Straightforward Enantioselective Synthesis of (+)-Ancistrofuran. *Tetrahedron* **2005**, *61* (40), 9545−9549.
(23) Wang, Y. X.; Yang, B.; Zhai, Y. Y.; Yin, Z.; Sun, Y. N.; Rao, Z. H. Peptidyl Aldehyde Nk-1.8k Suppresses Enterovirus 71 and Enterovirus 68 Infection by Targeting Protease 3c. *Antimicrob. Agents Chemother.* **2015**, *59*, 2636−2646.
(24) Ohtani, I.; Kusumi, T.; Kashman, Y.; Kakisawa, H. High-Field Ft Nmr Application of Mosher's Method. The Absolute Configurations of Marine Terpenoids. *J. Am. Chem. Soc.* **1991**, *113* (11), 4092−4096.
(25) Chang, H. K.; Shin, M. S.; Yang, H. Y.; Lee, J. W.; Kim, Y. S.; Lee, M. H.; Kim, J.; Kim, K. H.; Kim, C. J. Amygdalin Induces Apoptosis through Regulation of Bax and Bcl-2 Expressions in Human Du145 and Lncap Prostate Cancer Cells. *Biol. Pharm. Bull.* **2006**, *29* (8), 1597−1602.
(26) Cioni, J. P.; Doroghazi, J. R.; Ju, K. S.; Yu, X. M.; Evans, B. S.; Lee, J.; Metcalf, W. W. Cyanohydrin Phosphonate Natural Product from Streptomyces Regensis. *J. Nat. Prod.* **2014**, *77* (2), 243−249.
(27) Mitchell, B. L.; Bhandari, R. K.; Bebarta, V. S.; Rockwood, G. A.; Boss, G. R.; Logue, B. A. Toxicokinetic Profiles of Alpha-Ketoglutarate Cyanohydrin, a Cyanide Detoxification Product, Following Exposure to Potassium Cyanide. *Toxicol. Lett.* **2013**, *222* (1), 83−89.
(28) Chang, J.; Zhang, Y. Catalytic Degradation of Amygdalin by Extracellular Enzymes from Aspergillus Niger. *Process Biochem.* **2012**, *47* (2), 195−200.
(29) Ramalho, R. T.; Aydos, R. D.; Schettert, I.; de Assis, P. V.; Cassino, P. C. Sulfane Sulfur Deficiency in Malignant Cells, Increasing the Inhibiting Action of Acetone Cyanohydrin in Tumor Growth. *Acta Cir. Bras.* **2013**, *28* (10), 728−732.
(30) De Nicola, G. R.; Leoni, O.; Malaguti, L.; Bernardi, R.; Lazzeri, L. A Simple Analytical Method for Dhurrin Content Evaluation in Cyanogenic Plants for Their Utilization in Fodder and Biofumigation. *J. Agric. Food Chem.* **2011**, *59* (15), 8065−8069.
(31) Yokoi, Y. Pharmacological Studies of Some Organic Thiocyanates. *Jpn. J. Pharmacol.* **1954**, *3*, 99−111.
(32) Winiarski, L.; Oleksyszyn, J.; Sienczyk, M. Human Neutrophil Elastase Phosphonic Inhibitors with Improved Potency of Action. *J. Med. Chem.* **2012**, *55* (14), 6541−6553.
(33) Otwinowski, Z.; Minor, W. Macromolecular Crystallography. In *Methods in Enzymology*, Vol. *276*; Academic Press: New York, 1997; pp 307−326.
(34) Adams, P. D.; Grosse-Kunstleve, R. W.; Hung, L. W.; Ioerger, T. R.; McCoy, A. J.; Moriarty, N. W.; Read, R. J.; Sacchettini, J. C.; Sauter, N. K.; Terwilliger, T. C. Phenix: Building New Software for Automated Crystallographic Structure Determination. *Acta Crystallogr., Sect. D: Biol. Crystallogr.* **2002**, *58* (11), 1948−1954.
(35) Emsley, P.; Cowtan, K. Coot: Model-Building Tools for Molecular Graphics. *Acta Crystallogr., Sect. D: Biol. Crystallogr.* **2004**, *60* (12), 2126−2132.
(36) Laskowski, R.; MacArthur, M.; Moss, D.; Thornton, J. Procheck: A Program to Check the Stereochemical Quality of Protein Structures. *J. Appl. Crystallogr.* **1993**, *26*, 283−291.

DOI: 10.1021/acs.jmedchem.5b01013
J. Med. Chem. 2015, 58, 9414−9420